

An Approach for Optimal Measurements Selection on Gas Turbine Engine Fault Diagnosis

Min Chen¹

School of Energy and Power Engineering,
Beihang University,
Beijing 100191, China
e-mail: chenmin@buaa.edu.cn

Liang Quan Hu

Collaborative Innovation Center of Advanced
Aero-Engine,
Beijing 100191, China
e-mail: lovehulianguan@163.com

Hailong Tang

School of Energy and Power Engineering,
Beihang University,
Beijing 100191, China
e-mail: 75249612@qq.com

Gas path fault diagnosis plays an important role in guaranteeing safe, reliable and cost-effective operation for gas turbine engines. Measurements selection is among the most critical issues for diagnostic method implementation. In this paper, an integration approach for optimal measurements selection, which combines finger print diagrams analysis, health parameters correlation analysis, performance estimation uncertainty index analysis and fault cases validation based on genetic algorithm, has been proposed and applied to assess the health condition of a two-spool split flow turbofan in test bed. First, mathematical description of an engine gas path fault diagnosis process was given and the influence coefficient matrix was also calculated based on a well calibrated nonlinear engine performance simulation model. Second, the number of combination candidates was reduced from 782 to 256 and three measurements were picked out using the finger print diagrams analysis and the health parameters correlation analysis. Then, the number of the combination candidates was further narrowed down to 13 using the performance estimation uncertainty index analysis. A nonlinear genetic algorithm fault diagnosis method was applied to test the diagnostic ability of the remaining measurement candidates. Finally, an optimal measurement combination was worked out which demonstrated the effectiveness of the integration approach. This integration approach for optimal measurements selection is also applicable to other type of gas turbine engines. [DOI: 10.1115/1.4029171]

Keywords: two-spool split flow turbofan, gas path fault diagnosis, measurements selection, genetic algorithm

1 Introduction

Gas turbine engines are complex thermal equipment due to harsh operation environment. Engine gas path fault diagnosis plays an important role in ensuring reliable operation, reducing operating costs and prolonging service life. The idea of gas path fault diagnosis is based on the fact that any degradation in engine component performance results in a change of engine measurement. If the second change is traced, the degradation can be identified with gas path analysis. Thus, the engine diagnostic ability is not only determined by fault diagnosis methods but also by useful information the engine measurements contain.

A large variety of diagnostic methods for aero-engine gas path faults have been put forward in the previous literature. Generally, the existing methods can be divided into linear and nonlinear methods. Li provided an extensive review of these methods [1]. Based on the formation of an appropriate matrix called influence coefficient matrix, Doel [2] and Volponi [3] presented linear least square fault diagnosis method. Methods based on Kalman filtering have been presented by Provost [4] to distinguish faults between sensors and components. In order to consider the nonlinearity of engine behavior, a nonlinear model based method combined with conventional optimization was introduced by Stamatis et al. [5]. Unfortunately, conventional optimization is liable to get into local minimum. To overcome this limitation, genetic algorithm was applied to the nonlinear model based method by Zedda and Singh [6] in the past 15 years.

No matter which diagnostic method is chosen, one critical issue to determine the diagnostic effectiveness is the useful information

measurements contain. This issue seems to be more important especially at the stage of designing or manufacturing a new engine [7]. It is due to the fact that the decision for instrumenting an engine has to be taken in order to ensure a good capability of in-service monitoring.

In theory, more measurements are chosen, more effective information is available. Ideally, engine measurements can be obtained by placing sensors at the inlet and outlet sections of each component to get a full picture of the change that a component causes to working fluid. However, such an approach is not practical for several reasons [8]. First, it is very expensive and complex to place so many sensors in an engine. Second, the inclusion of sensors such as thermocouples, wall taps and pitot probes causes flow disturbances. Third, measurements may not be obtained at some locations because of harsh local conditions (for example, at the high pressure turbine (HPT) inlet). It is thus desirable to use a minimum number of measurements without sacrificing the diagnostic ability.

In the past years, several methods related to measurements selection have been put forward by different scholars. Sensitivity analysis was first applied by Stamatis et al. [5]. They put forward some criteria for optimal measurements selection and health parameters selection. In later years, Provost [4,9] employed correlation matrix to examine the degree of measurements interdependence. Mathioudakis and Kamboukos [7] and Kamboukos et al. [8] used a method based on the condition number of Jacobian matrix for optimal measurements selection. Stamatis et al. [5] applied performance estimation uncertainty index method to perform a check on the values of measurements. Jasmani [10] developed analytical methodology combined with sensitivity analysis, correlation analysis and subset concept to select measurements. Simon [11] constructed a performance metric which was defined as function of the steady state error covariance and the cost of selected sensors.

¹Corresponding author.

Contributed by the Aircraft Engine Committee of ASME for publication in the JOURNAL OF ENGINEERING FOR GAS TURBINES AND POWER. Manuscript received September 1, 2014; final manuscript received November 8, 2014; published online December 23, 2014. Editor: David Wisler.

To perform the sensors selection, Borguet [12] put forward a metric which combined the essential elements of the selection problem. It included the condition number, the trace and the determinant of Fisher information matrix, which can both measure the global sensitivity of sensors with respect to the health parameters and the overall uncertainty on the estimated parameters. Michael [13] put forward systematic sensors selection strategy. It provided a procedure for quantifying the value of candidate sensors based on criteria including speed of fault detection, probability of correct fault source isolation, and overall risk reduction potential. It was rather applied to rocket engines than aero-engines.

However, from the literature stated above, a measurements selection criterion based on engine health parameters correlation rather than measurements correlation has not been reported. In addition, no one has answered whether this method based on health parameters correlation can be integrated with other methods to provide a universal and efficient way for optimal measurements selection.

In this paper, we mainly focus on a novel combined approach for optimal measurements selection on aero-engine gas path fault diagnosis especially used in test bed. The remainder of this paper is organized as follows. Section 2 describes mathematical description of an aero-engine gas path fault diagnosis process. Section 3 specifies the method of optimal measurements selection. Then, in Sec. 4 experimental results were given to verify the effectiveness of the proposed approach. Our concluding remarks are contained in Sec. 5.

2 Fault Diagnosis Method Description

2.1 Mathematical Description. For the purpose of gas path fault diagnosis, engine is considered as a system. Its thermodynamic relationship can be expressed with the following equation:

$$y = g(u, x) \quad (1)$$

In this equation, engine operating condition is defined by means of a set of variables, denoted as vector u . Engine component health condition is represented through the values of a set of appropriate health parameters, denoted as vector x . The system is observed through a set of measurements, denoted as vector y . $g(\cdot)$ is a vector-valued function representing engine thermodynamic behavior.

For a given operating point u , the measurements only depend on the health condition of engine components. It can be expressed with the following equation:

$$y = g(x) \quad (2)$$

When an engine is in health condition, both the health parameters and the measurements have the reference values

$$y^{\text{ref}} = g(x^{\text{ref}}) \quad (3)$$

In the frame of gas path fault diagnosis, the formula is rarely used in the form denoted as Eq. (1). Instead, what we are concerned about most is the deviation between the actual values and the reference values corresponding to a healthy engine. In general, the functional relationship between the deviation of measurements vector δy and the deviation of component health parameters vector δx is nonlinear. However, if deviations are small, a linear functional relationship can be used to link them together. Then, Eq. (2) may transform into the following equation:

$$\delta y = G \delta x \quad (4)$$

where

$$G = \frac{\partial}{\partial x} g(x) \quad (5)$$

is influence coefficient matrix of the engine model at the linearization point, also named Jacobian matrix.

In order to account for the effect of measurement noise, a vector $v \in N(0, R_y)$ is added to the deterministic linearized model in order to reconcile the observed measurements and the predictions. Therefore, Eq. (4) transforms into the following equation:

$$\delta y = G \delta x + v \quad (6)$$

Equation (6) can further be scaled to a linear system with a noise distribution $\tilde{v} \in N(0, I)$ provided that the covariance matrix \tilde{R}_y is positive definite. The scaled model [14] is given by

$$\tilde{G} = \left(\sqrt{\tilde{R}_y} \right)^{-1} G \quad (7)$$

where the scaling factor takes into account the relative accuracy of each sensor.

There may be several orders of magnitude difference between the values in different columns of \tilde{G} . In order to scale all columns of the Jacobian matrix into the same magnitude to prevent the large matrix elements from dominating, one can compute the magnitude of each column g_i of \tilde{G} as $g_i^T g_i$ [15]. Premultiply \tilde{G} by

$$W = \begin{bmatrix} \sqrt{g_1^T g_1} & 0 & 0 \\ 0 & \ddots & 0 \\ 0 & 0 & \sqrt{g_m^T g_m} \end{bmatrix}^{-1} \quad (8)$$

Let us define

$$\tilde{W} = \tilde{G} W \quad (9)$$

After the aforementioned transformation, each column of \tilde{W} has the same magnitude. It has to be noted that this transformation matrix forms the base for the following methods including finger print diagrams analysis, health parameters correlation analysis and performance estimation uncertainty index analysis.

2.2 Aero-Engine Performance Modeling. In order to work out the transformation matrix \tilde{W} , a two-spool split flow turbofan was chosen as a test case. The model engine was a newly design engine still in test bed. The engine layout is shown in Fig. 1.

The engine performance was simulated on an open object-oriented engine performance platform [16,17] developed by Beihang University, People's Republic of China. It has been calibrated by test bed data at fixed operating conditions ($H=0$, $Ma=0$, $N1=100\%$). Some basic engine performance parameters are shown in Table 1.

Base on Fig. 1, there are four major engine rotating components being diagnosed as follows:

- (1) fan (FAN)
- (2) high pressure compressor (HPC)
- (3) HPT
- (4) low pressure turbine (LPT)

For each rotating component, it needs two health parameters, i.e., efficiency index and flow capacity index to indicate its health condition, which are defined as follows:

$$\begin{aligned} \text{efficiency index: } E_i &= \eta_{\text{act}} / \eta_{\text{ref}} \\ \text{flow capacity index: } W_i &= \left(W \sqrt{\theta} / \delta \right)_{\text{act}} / \left(W \sqrt{\theta} / \delta \right)_{\text{ref}} \end{aligned}$$

The set of health parameters for these four rotating components is shown in Table 2.

In the test bed, there are 12 possible measurement candidates through placing corresponding sensors at the engine sections. The measurements candidates and their standard deviations are shown in Table 3.

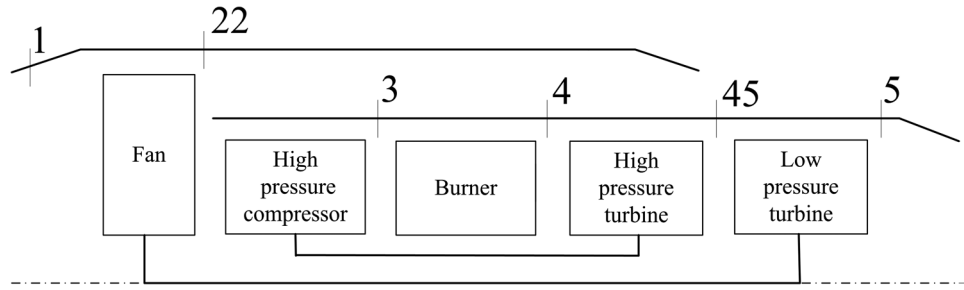


Fig. 1 Two-spool split flow turbofan structure diagram

Table 1 Target engine performance parameters

Design parameters	Value
Total pressure ratio	7.5
Bypass ratio	1.6
Intake total air flow rate	6.3 kg/s
High turbine entry temperature	1350 K

Table 2 Health parameters for target engine

No.	Component health parameters	Symbol
1	FAN efficiency index	E_1
2	FAN flow capacity index	W_1
3	HPC efficiency index	E_2
4	HPC flow capacity index	W_2
5	HPT efficiency index	E_3
6	HPT flow capacity index	W_3
7	LPT efficiency index	E_4
8	LPT flow capacity index	W_4

Table 3 Measurement candidates for the target engine

No.	Symbol	Engine measurement candidates	Standard deviation (%)
1	T22	FAN outlet total temperature	0.2
2	P22	FAN outlet total pressure	0.3
3	T3	HPC outlet total temperature	0.2
4	P3	HPC outlet total pressure	0.3
5	T45	HPT outlet total temperature	0.5
6	P45	HPT outlet total pressure	0.3
7	T5	LPT outlet total temperature	0.2
8	P5	LPT outlet total pressure	0.3
9	N2	HPC rotational speed	0.1
10	WA	Total air flow rate	0.5
11	WF	Fuel flow rate	0.3
12	F	Thrust	0.8

Table 4 Engine influence coefficient matrix ($H = 0$, $Ma = 0$, $N1 = 100\%$)

	E_1	W_1	E_2	W_2	E_3	W_3	E_4	W_4
T22	-0.0785	0.0443	-0.0325	-0.0092	-0.0342	0.0302	0.0143	-0.0453
P22	0.0318	0.1284	-0.0666	-0.0227	-0.0702	0.0619	0.0377	-0.1339
T3	-0.2089	0.1368	-0.1917	-0.0753	0.0401	-0.1494	-0.1008	0.1859
P3	-0.2622	0.3259	-0.0015	-0.0012	0.0205	-0.3371	-0.2319	0.3317
T45	-0.1687	0.1107	-0.1984	-0.0625	-0.2117	0.1868	-0.1889	0.0141
P45	-0.2665	0.3261	-0.0171	0.0011	-0.0145	0.0098	-0.3149	0.1146
T5	-0.4346	0.2849	-0.5109	-0.1607	-0.5442	0.4765	-0.5458	0.1072
P5	-0.2839	0.3373	-0.0371	-0.0048	-0.0357	0.0222	-0.2883	0.3382
N2	-0.4437	0.4954	0.7229	-0.9758	0.7081	-0.6998	-0.2378	0.7538
WA	-0.0027	0.1154	0.0063	0.0023	0.0078	-0.0065	-0.0032	0.0082
WF	-0.5539	0.5074	-0.3631	-0.1077	-0.3835	0.3285	-0.5953	0.3508
F	-0.0886	0.1653	-0.0351	-0.0094	-0.0357	0.0298	-0.0886	0.0736

It has to be noted that thrust and total air flow rate were among the candidates since the target engine in this paper was still in test bed and these two parameters were available. If the target engine is installed on wing, these two candidates should be excluded from the table.

It has to be noted that the interturbine temperature T45 in this test case does not exceed 1150 K. Based on the current technology level, it is not difficult to sense the temperature and pressure at this position. Therefore, T45 and P45 were also among the candidates.

Using the developed engine model, the influence coefficient matrix G can be determined by implanted individually 1% deviation from the referenced one, toward each component health parameters. Measurement noise standard deviations [18,19] (shown in Table 3) were added to transform the matrix G . Based on Eqs. (7)–(9), it transformed into influence coefficient matrix \tilde{W} , which is shown in Table 4.

3 Measurements Selection Process

Just as mentioned above, eight component health parameters and twelve-measurement candidates are available in the test case. Mathematically, at least eight measurements are required in order that all these health parameters are uniquely estimated [20]. All possible combinations can be chosen using K-choose-M combinatorial approach, where K means the total available measurements. The largest number of measurements is not necessarily the best measurements considering the factors such as sensor costs, ease of sensor integration, the potential close correlation between the measurements and so on. In this test case, K is 12 and the possible number of M can be 8, 9, 10, 11, and 12. Then, the total available number of measurement combinations is shown below:

$$C_{12}^8 + C_{12}^9 + C_{12}^{10} + C_{12}^{11} + C_{12}^{12} = 782 \quad (10)$$

In order to effectively select the optimal measurements, a combined method is presented and described here in detail. It includes finger print diagrams analysis, health parameters correlation analysis and performance estimation uncertainty index analysis and

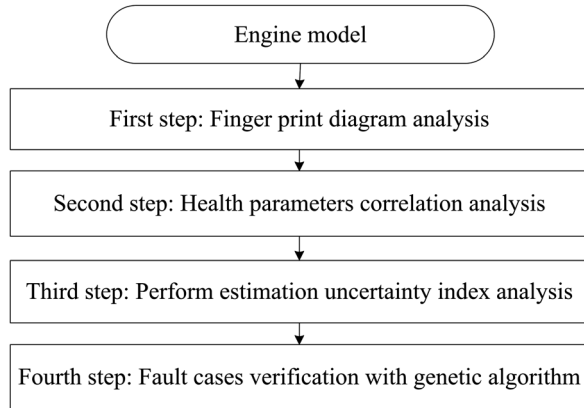


Fig. 2 Flow chart of measurements selection process

fault cases verification with genetic algorithm. The flow chart of the measurements selection process is shown in Fig. 2.

3.1 Finger Print Diagrams Analysis. Using the data of each column from Table 4, finger print diagram for each measurement can be easily plotted. It can obviously indicate the influence of a particular measurement caused by the same perturbation of each component health parameter. One example is shown in Fig. 3. There are totally twelve diagrams since twelve-measurement candidates are available in this test case.

The criterion for measurements selection in this step is that a particular measurement can be selected if it is far more sensitive to a health parameter than all the other health parameters.

From Fig. 3, it can be seen that the influence of component health parameter W_1 on the measurement total air flow rate (WA) is far stronger than the other parameters. Therefore, WA should be chosen since it can distinguish the health parameter W_1 from the other health parameters. After analyzing the other eleven diagrams, no other measurements can meet the criterion stated above. In conclusion, only WA can be selected in this step.

3.2 Health Parameters Correlation Analysis. From the previous literature, little attention has been paid to the health parameters correlation analysis. However, it is an effective way to discriminate similar gas path engine faults. Different from deselecting measurements through measurements correlation analysis by Provost [4,9], in this step, health parameters correlation analysis is applied to measurements selection. The criterion lies in that a particular measurement must be selected if its deviation is

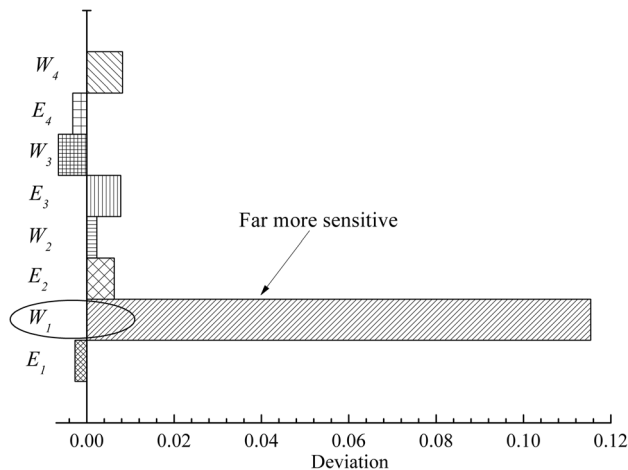


Fig. 3 Total air flow rate (WA) finger print diagram

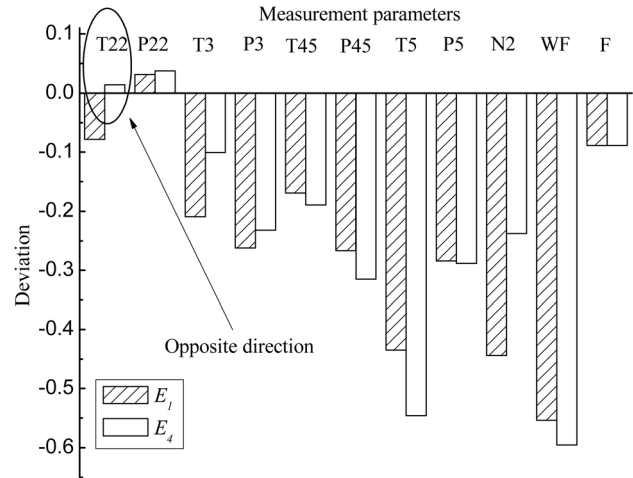


Fig. 4 Correlation analysis diagram between E_1 and E_4

responded in opposite direction by any two different health parameters with high correlation degree.

The correlation degree of any two health parameters can be reflected by correlation coefficient R_{UV} defined as follows:

$$R_{UV} = \cos \theta = \frac{U^T V}{\|U\|_2 \|V\|_2} \quad (11)$$

where U and V are two column vectors of Table 4.

The closer the value of R_{UV} is to one, the more relevant are the two column vectors. In other words, these two health parameters are similar and they are difficult to be identified. In order to identify these similar health parameters, one should select the measurements whose trends are responded in opposite direction by the health parameters.

There are totally $28(C_8^2 = 28)$ column combinations when one, respectively, calculate R_{UV} between any two different columns in Table 4. Particularly, below are two combinations whose R_{UV} is greater than 0.95:

- (1) $(E_1, E_4) R_{UV} = 0.972$
- (2) $(E_2, E_3) R_{UV} = 0.959$

It means that (E_1, E_4) is highly relevant and difficult to be identified from each other. The same applied to (E_2, E_3) . In order to identify them effectively, one should first find the difference from the correlation diagrams. Figures 4 and 5 present the correlation diagrams between health parameters (E_1, E_4) , (E_2, E_3) , respectively.

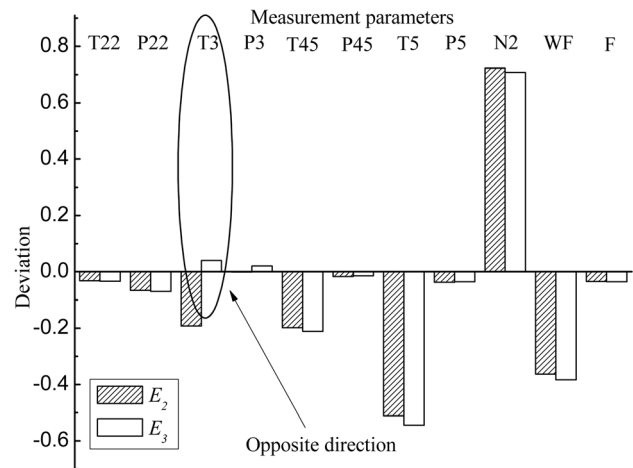


Fig. 5 Correlation analysis diagram between E_2 and E_3

Table 5 Measurement combinations with lowest J -value

No.	Number of measurement parameters	WA	T22	T3	P22	P3	T45	P45	T5	P5	N2	WF	F	$\lg J$
1	8	•	•	•		✓		✓	✓	✓	✓			0.915
2		•	•	•		✓		✓	✓		✓	✓		0.926
3		•	•	•		✓	✓	✓		✓	✓			0.930
4	9	•	•	•	✓	✓		✓	✓	✓	✓			0.856
5		•	•	•	✓	✓		✓	✓		✓	✓		0.866
6		•	•	•	✓	✓		✓		✓	✓	✓		0.876
7	10	•	•	•	✓	✓		✓	✓	✓	✓	✓		0.841
8		•	•	•	✓	✓	✓	✓	✓	✓	✓			0.852
9		•	•	•	✓	✓	✓	✓	✓	✓	✓			0.857
10	11	•	•	•	✓	✓		✓	✓	✓	✓	✓	✓	0.838
11		•	•	•	✓	✓	✓	✓	✓	✓	✓	✓		0.843
12		•	•	•	✓	✓	✓	✓	✓	✓	✓		✓	0.848
13	12	•	•	•	✓	✓	✓	✓	✓	✓	✓	✓	✓	0.835

From Fig. 4, it can be seen that if one wants to identify E_1 from E_4 , measurement T22 must be selected because its trend is responded in opposite direction by the faults. Similarly, T3 must be selected if one wants to identify E_2 from E_3 (shown in Fig. 5).

To sum up, on the basis of health parameters correlation analysis, measurements T22 and T3 were selected in this step.

3.3 Performance Estimation Uncertainty Index Analysis.

From the finger print diagrams analysis and the health parameters correlation analysis stated above, three measurements have been selected including WA, T22, and T3. However, it is not enough for engine gas path analysis since the number of measurements should be no less than the number of health parameters. In this test case, the number of measurements should be no less than eight. Thus, at least five measurements have to be picked out from the remaining nine measurement candidates. Then, the total number of measurement combinations was calculated as below:

$$C_9^5 + C_9^6 + C_9^7 + C_9^8 + C_9^9 = 256 \tag{12}$$

To further selection of the other measurements, performance estimation uncertainty index analysis [21] was chosen in this step.

The least square estimate of δx allowing for measurement noise was given by [21]

$$\delta x = (\tilde{W}^T \tilde{R}_y^{-1} \tilde{W})^{-1} \tilde{W}^T \tilde{R}_y^{-1} \delta y \tag{13}$$

where \tilde{W} is the influence coefficient matrix shown in Eq. (9), \tilde{R}_y is the measurement covariance matrix

$$\tilde{H} = \tilde{W}^T \tilde{R}_y^{-1} \tilde{W} \tag{14}$$

where \tilde{H} is called information matrix

In order to evaluate the estimate effectiveness, performance estimation uncertainty index is presented as follows [21]:

$$J = (\text{tr}(\tilde{H}^{-1})/M)^{1/2} \tag{15}$$

J is named performance estimation uncertainty index, where $\text{tr}(\cdot)$ is the trace of \tilde{H}^{-1} which is the sum of diagonal elements. M is the number of measurements.

The value of J (also named J -value) is a kind of global root mean square error for the information matrix [21]. Clearly, the smaller the J -value, the more accurate is the estimate. It indicates the amount of useful information that the measurement combinations contain. Therefore, it can be used as a criterion for narrowing the range of the measurement combinations.

From Eq. (12), there are 256 measurement combinations. According to the number of measurements, all these measurement combinations are divided into five groups (from group A to group E). For example, all the eight-measurement combinations are put into group A and twelve-measurement combinations are put into group E.

In each group, J -values of all the measurement combinations were calculated one by one and sorted. For each group, the best three sets of measurement combinations with lowest J -value were picked out for further validation. Table 5 presents 13 typical sets of measurement combinations picked out from the five groups. In the table, symbol "•" indicates the selected measurements in the previous steps. Symbol "✓" indicates the selected measurements using performance estimation uncertainty index analysis.

Until this step, still unknown whether all these selected combinations are able to identify the common engine gas path faults. Validation with typical fault cases is necessary to obtain the best measurement combination. The method used in the fourth step was genetic algorithm.

3.4 Validation Process Using Genetic Algorithm

3.4.1 Brief Introduction of Genetic Algorithm. Genetic algorithm follows the idea of Darwin's natural evolution and is one of the optimization searching techniques [22,23]. Compared with the conventional optimization methods, longer computation time is the main drawback of genetic algorithm. However, this penalty can be minimized with the advent of super parallel computing technology. In addition, it offers several unique features. It can combine elements of directed and stochastic search. It is also a global search to avoid getting stuck in local optima. Even non-smooth functions can be optimized since no derivatives are required. Due to these features, genetic algorithm is used as the validation method here.

Genetic algorithm optimization steps normally include encoding, decoding, fitness evaluation, selection, crossover and mutation. Considering the nonlinear feature of the engine model as well as searching for a better solution, an adaptive genetic algorithm was utilized in this step. The uniqueness of this algorithm is that it can automatically change the probability of crossover and mutation when the fitness is greater than the average fitness [22].

3.4.2 Genetic Algorithm Procedure. Measurement combinations validation can be regarded as searching the best solution for an optimization problem with the help of genetic algorithm. Its idea is shown in Fig. 6. For each measurement combination, calculated measurements \hat{y}_i are compared with target measurements \bar{y}_i . The difference between $\hat{y}_i - \bar{y}_i$ is used by genetic algorithm to update the estimation of the component health parameters \hat{x}_i . Any

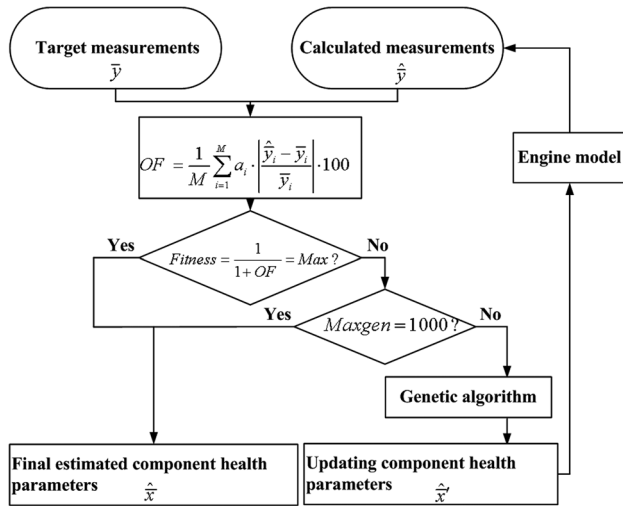


Fig. 6 Measurement combinations validation using genetic algorithm

potential solution \hat{x}_i is evaluated by means of an objective function (OF) [23] defined in the following equation:

$$OF = \frac{1}{M} \sum_{i=1}^M a_i \cdot \left| \frac{\bar{y}_i - \hat{y}_i}{\bar{y}_i} \right| \cdot 100 \quad (16)$$

where a_i is weighting factors of the measurements taking into account the measurement noise [6,24].

Generally, \bar{y}_i is the measured value vector from the real engine component fault cases. If such fault cases are unavailable, it can be obtained through deliberately implanting component performance degradation and adding measurement noise X_{noise} into a well calibrated engine model. Component degradation can be set through perturbing the value of component health parameters. For example, 1% of decrease in health parameter E_1 means 1% efficiency degradation in fan component. Measurement noise is usually assumed to be Gaussian distribution with mean $\mu_i = 0$. Relative value of X_{noise} [25] is defined in the following equation:

$$X_{noise} = R(\mu_i + 3\sigma_i) \quad (17)$$

where R is a random number between $[-1, 1]$.

A fitness defined in Eq. (16) is used to represent the quality of any potential solution [25] and it is maximized in the genetic algorithm searching process to achieve best possible solution. A value of fitness approaching one indicates a good solution while a value of fitness approaching zero indicates a poor solution.

$$Fitness = \frac{1}{1 + OF} \quad (18)$$

3.4.3 Genetic Algorithm Implementation. Genetic algorithm operating parameters were set initially as follows: (1) population size, $Popsize = 100$, (2) number of generation, $Maxgen = 2000$, (3) probability of crossover, $P_c = 0.75$, (4) probability of mutation, $P_m = 0.05$, (5) probability of adaptive crossover, $P_{c1} = 0.9$, $P_{c2} = 0.6$, and (6) probability of adaptive mutation, $P_{m1} = 0.1$, $P_{m2} = 0.001$.

Considering the stochastic feature of genetic algorithm and better operating efficiency, the optimal search process can be adjusted as follow. First, the top five solutions with max fitness are selected and stored initially in the first generation. If the solution in the next generation has greater fitness than the last one, the solution with less fitness is replaced by the one with higher fitness. Second, the same operation is repeated until it reaches the maximum generation or it reaches the maximum fitness. Finally, the top five solutions

with highest fitness in the whole generation, as well as their corresponding estimate of engine component health parameters are obtained. The average of the five estimates is the final solution.

4 Results Analysis

As to the compression components (FAN and HPC), blade fouling results in the decrease of efficiency and the flow capacity [10]. In this test case, the decrease of compression components efficiency and the flow capacity were assumed to be -1% and -3% , respectively. For the expansion components (HPT and LPT), blade erosion was used as the test case with assumed deviations of -1% in efficiency and $+3\%$ in flow capacity. These component degradations were implanted into engine performance model to simulate measurements of degraded engine for gas path analysis.

To validate the faults identification effectiveness of the measurement combinations, 15 component fault cases were chosen in Table 6. They included single component fault cases, two components fault cases, three components fault cases and four components fault cases. These 15 component fault cases are sufficient to cover most common rotating component faults occurrence in the target engine.

All these fifteen typical fault cases were validated with the above genetic algorithm method using the thirteen different measurement combinations. The diagnostic accuracies are gauged based on the fitness shown in Eq. (18). The closer the fitness is to one, the higher the diagnostic accuracies are. Comparison of diagnostic accuracies for the fault cases using the different measurement combinations is shown in Table 7. From the table, some useful conclusions can be drawn as follows:

- (1) Allowing for measurement noise effect, all the fitness values are greater than 0.87. It can be concluded that the identification accuracies are within the acceptable range and the genetic algorithm is robust.
- (2) The No. 2 measurement combination (the highlight column in the table) is the only one combination whose fitness values of all the fifteen typical fault cases are greater than 0.905. Its fitness values rank No. 1 (largest) in most fault cases except fault cases 3, 7, 12, and 13. It demonstrates super diagnostic ability among all the measurement combinations. The measurements in this combination include WA, T22, T3, P3, P45, T5, N2, and WF.

Figures 7–10 also presents the genetic algorithm identification results for single component fault to four components faults, respectively, using the No. 2 measurement combination. In the figures, "mesh bar" means the implanted component degradations, the adjacent "blank bar" means the genetic algorithm identification results. The lower is the height difference between these two bars, the higher is the diagnostic accuracy. From these figures, it

Table 6 Component fault cases

No. of fault case	No. of component	Degraded components
1	1	FAN
2	1	HPC
3	1	HPT
4	1	LPT
5	2	FAN + HPC
6	2	FAN + HPT
7	2	FAN + LPT
8	2	HPC + HPT
9	2	HPC + LPT
10	2	HPT + LPT
11	3	FAN + HPC + HPT
12	3	FAN + HPC + LPT
13	3	FAN + HPT + LPT
14	3	HPC + HPT + LPT
15	4	FAN + HPC + HPT + LPT

Table 7 Fitness of measurement combinations in different fault cases

No. of fault cases	No. of measurement combinations													
	1	2	3	4	5	6	7	8	9	10	11	12	13	
1	0.873	0.908	0.900	0.905	0.898	0.904	0.897	0.910	0.892	0.906	0.904	0.902	0.894	
2	0.921	0.927	0.884	0.907	0.882	0.912	0.915	0.895	0.912	0.908	0.907	0.895	0.913	
3	0.894	0.905	0.903	0.890	0.902	0.898	0.913	0.906	0.903	0.900	0.884	0.885	0.887	
4	0.905	0.922	0.877	0.875	0.915	0.905	0.910	0.912	0.903	0.887	0.907	0.911	0.912	
5	0.885	0.902	0.902	0.900	0.896	0.906	0.892	0.911	0.896	0.876	0.897	0.912	0.895	
6	0.906	0.915	0.898	0.903	0.886	0.877	0.906	0.900	0.907	0.889	0.894	0.906	0.905	
7	0.899	0.909	0.905	0.901	0.905	0.891	0.905	0.894	0.910	0.917	0.906	0.886	0.885	
8	0.912	0.920	0.895	0.898	0.913	0.908	0.895	0.910	0.889	0.917	0.913	0.905	0.914	
9	0.901	0.915	0.904	0.906	0.909	0.911	0.897	0.901	0.895	0.896	0.897	0.891	0.896	
10	0.910	0.917	0.899	0.911	0.897	0.907	0.915	0.883	0.911	0.902	0.913	0.903	0.901	
11	0.912	0.910	0.901	0.896	0.901	0.883	0.898	0.898	0.905	0.906	0.902	0.905	0.902	
12	0.904	0.915	0.900	0.898	0.909	0.908	0.901	0.911	0.906	0.905	0.907	0.888	0.910	
13	0.901	0.907	0.911	0.902	0.900	0.897	0.897	0.904	0.892	0.893	0.895	0.904	0.893	
14	0.896	0.909	0.893	0.894	0.895	0.885	0.903	0.887	0.915	0.907	0.900	0.894	0.897	
15	0.907	0.912	0.907	0.903	0.903	0.901	0.909	0.903	0.899	0.893	0.897	0.902	0.904	

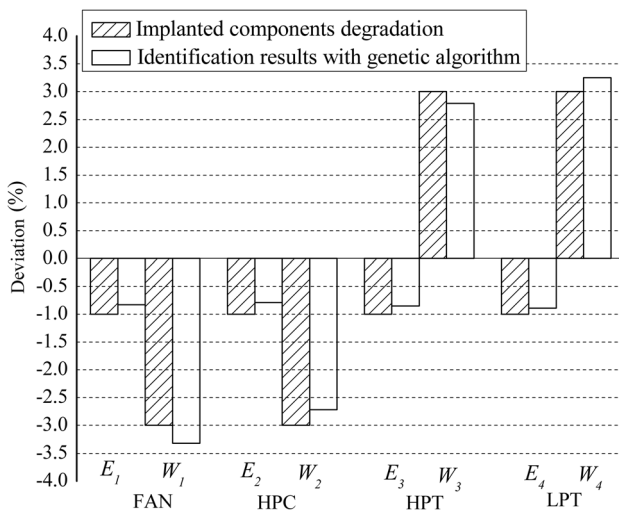


Fig. 7 Single component fault identification results

can be seen that the identification results are acceptable although slight difference can be found in these figures.

It should also be noted that combinations 4–13 has more measurements than combinations 1–3. More measurements mean high

fault diagnosis costs. Taking into account the diagnostic ability and cost, the No. 2 combination was the recommended measurement combination including eight measurements WA, T22, T3, P3, P45, T5, N2, and WF. This combination cannot only produce higher accuracy in identifying the engine component faults but also can reduce the fault diagnosis costs.

In order to demonstrate the validity of this integration approach, a further numerical experiment was done. In this experiment, the first two steps finger print diagrams analysis and health parameters correlation analysis were skipped and the third step performance estimation uncertainty index analysis(also named one-step method) was utilized directly to search the optimal measurement combination globally out of the total 792 candidates.

From Table 8 shown below, it can be seen that the best three eight-measurement combinations selected from the one-step method are different from the ones based on the method put forward in this manuscript(also named three-step method). To compare the faults identification effectiveness with these two methods, genetic algorithm method was also utilized to identify the fifteen typical component fault cases (shown in Table 6). The diagnostic accuracies can be determined based on the genetic algorithm average fitness of the typical fault cases. The closer the average fitness is to one, the higher the diagnostic accuracy is.

Table 9 presents the fitness of eight-measurement combinations from different selection methods. It can be seen that the best three measurement combinations from the three-step method have the

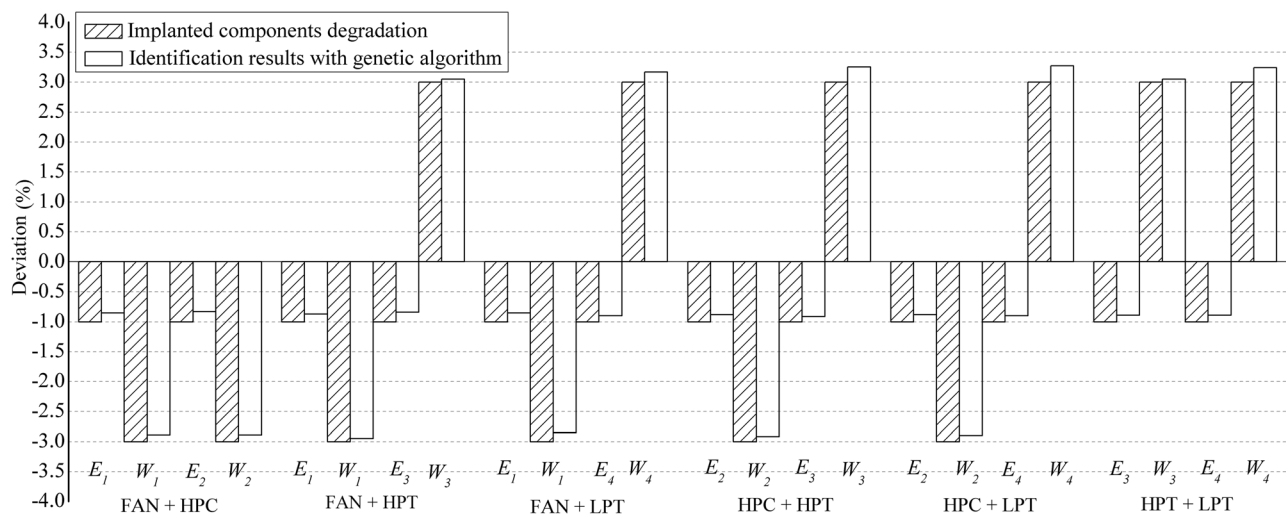


Fig. 8 Two components faults identification results

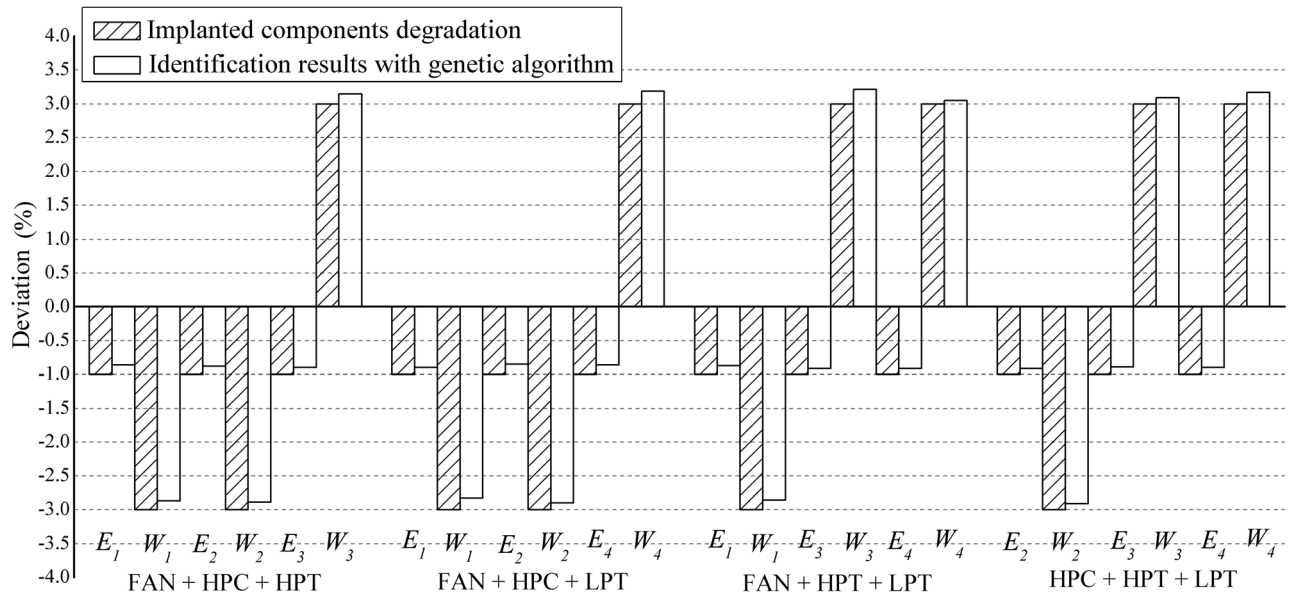


Fig. 9 Three components faults identification results

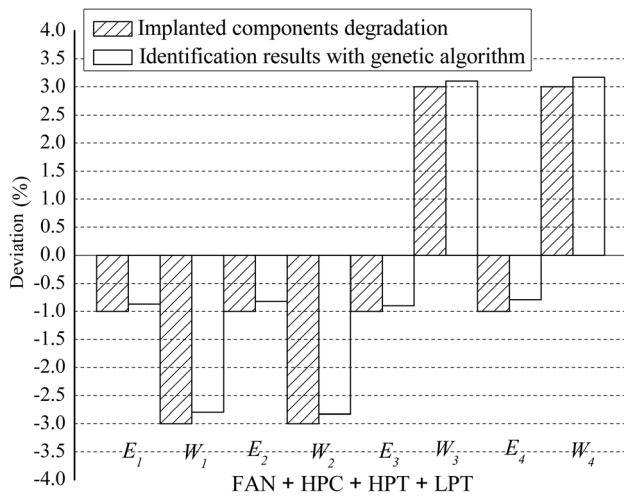


Fig. 10 Four components faults identification results

Table 8 The best three eight-measurement combinations from different selection methods

No.	Method	WA	T22	T3	P22	P3	T45	P45	T5	P5	N2	WF	F	lgJ
1	One-step method	✓	✓	✓	✓	✓	✓	✓	✓	✓	✓	✓	✓	0.867
2		✓	✓	✓	✓	✓	✓	✓	✓	✓	✓	✓	✓	0.884
3		✓	✓	✓	✓	✓	✓	✓	✓	✓	✓	✓	✓	0.889
1	Three-step method	✓	✓	✓	✓	✓	✓	✓	✓	✓	✓	✓	✓	0.915
2		✓	✓	✓	✓	✓	✓	✓	✓	✓	✓	✓	✓	0.926
3		✓	✓	✓	✓	✓	✓	✓	✓	✓	✓	✓	✓	0.930

highest average fitness (0.902, 0.913, and 0.899, respectively) than the ones from the one-step method (0.875, 0.869, and 0.872, respectively). It indicates that higher diagnostic accuracy can be obtained using the three-step measurements selection method. Therefore, the first two steps in this manuscript cannot be skipped in order to select the optimal measurements selection.

5 Conclusions

In this paper, an integration approach for optimal measurements selection has been presented for the aero-engine gas path fault

Table 9 Fitness of eight-measurement combinations from different selection methods

	No. of measurement parameter combinations	No. of measurement parameter combinations					
		Three-step method			One-step method		
		1	2	3	1	2	3
No. of fault case	1	0.873	0.908	0.900	0.876	0.867	0.874
	2	0.921	0.927	0.884	0.879	0.870	0.869
	3	0.894	0.905	0.903	0.875	0.868	0.873
	4	0.905	0.922	0.877	0.870	0.871	0.872
	5	0.885	0.902	0.902	0.873	0.870	0.873
	6	0.906	0.915	0.898	0.873	0.867	0.874
	7	0.899	0.909	0.905	0.876	0.870	0.869
	8	0.912	0.920	0.895	0.874	0.871	0.870
	9	0.901	0.915	0.904	0.874	0.866	0.877
	10	0.910	0.917	0.899	0.877	0.871	0.870
	11	0.912	0.910	0.901	0.877	0.868	0.871
	12	0.904	0.915	0.900	0.880	0.867	0.872
	13	0.901	0.907	0.911	0.875	0.870	0.871
	14	0.896	0.909	0.893	0.871	0.868	0.875
	15	0.907	0.912	0.907	0.874	0.871	0.870
Average fitness		0.902	0.913	0.899	0.875	0.869	0.872

diagnosis in test bed. Through the research, some useful conclusions are obtained:

- (1) Finger print diagrams analysis for health parameters provides a fast way to discover the most unique measurements for the particular engine component degradation.
- (2) How to discriminate similar health parameters is critical to increase the fault diagnostic success rate. Health parameters correlation analysis is an efficient way to pick out the measurements to distinguish similar engine faults with high correlation.
- (3) Performance estimation uncertainty index analysis can narrow the range of the measurement combinations by evaluating the useful information that the measurements contain.
- (4) The genetic algorithm identification results, for single component fault to multiple components faults using the No. 2 measurement combination WA, T22, T3, P3, P45, T5, N2, and WF, are within the acceptable range. The identification

accuracy can be further increased through future research on improved genetic algorithm.

- (5) The four-step integration approach provides a useful and universal tool to simplify the measurements selection process for different type gas turbine engines fault diagnosis.

Acknowledgment

This work was supported by the Natural Science Foundation of China (NSFC) under Grant No. 51206005. It was also supported by Beijing Youth Talent Plan and the Fundamental Research Funds for the Central Universities.

Nomenclature

- $g()$ = vector-valued function
 G, \tilde{G}, \tilde{W} = influence coefficient matrix
 H = altitude
 I = unit matrix
 Ma = Mach number
 $N1$ = low pressure spool relative rotational speed
 $N(m, R)$ = a Gaussian probability density function with mean m and covariance R
 R_y = covariance
 \tilde{R}_y = covariance matrix
 u = operating condition vector
 v = measurement noise vector
 $(W\sqrt{\theta}/\delta)_{act}$ = actual corrected flow
 $(W\sqrt{\theta}/\delta)_{ref}$ = referenced corrected flow
 x = component health parameters vector
 \hat{x} = estimated component health parameters vector
 y = measurements vector
 \bar{y} = target measurements vector
 \tilde{y} = simulated measurements vector
 η_{act} = actual efficiency
 η_{ref} = referenced efficiency
 σ = standard deviation

Subscript

- 1–5 = aero-engine gas path station number (shown in Fig. 1)

Superscripts

- T = transpose
 –1 = inverse

References

- [1] Li, Y. G., 2002, "Performance-Analysis-Based Gas Turbine Diagnosis: A Review," *Proc. Inst. Mech. Eng., Part A*, **216**(A6), pp. 363–377.
 [2] Doel, D. L., 1993, "Gas Path Analysis-Problem and Solution," 17th Symposium of Aircraft Integrated Monitoring Systems, Bonn, Germany, Sept. 21–23, pp. 21–23.
 [3] Volponi, A. J., 1982, "Gas Path Analysis: An Approach to Engine Diagnostics," 35th Symposium Mechanical Failures Prevention Group, Gaithersburg, MD, Apr. 20–22, pp. 10–18.
 [4] Provost, M. J., 1995, "The Use of Optimal Estimation Techniques in the Analysis of Gas Turbine," Ph.D. thesis, Cranfield University, Cranfield, UK.
 [5] Stamatias, M., Mathioudakis, K., and Papailiou, K., 1992, "Optimal Measurement and Health Index Selection for Gas Turbine Performance Status and Fault Diagnosis," *ASME J. Gas Turbines Power*, **114**(2), pp. 209–216.
 [6] Zedda, M., and Singh, R., 1999, "Gas Turbine Engine and Sensor Fault Diagnosis Using Optimization Techniques," *AIAA Paper No. 99-2530*.
 [7] Mathioudakis, K., and Kamboukos, P., 2006, "Assessment of the Effectiveness of Gas Path Diagnosis Schemes," *ASME J. Gas Turbines Power*, **128**(1), pp. 57–63.
 [8] Kamboukos, P., Oikonomou, P., Stamatias, A., and Mathioudakis, K., 2001, "Optimizing Diagnostic Effectiveness of Mixed Turbofans By Means of Adaptive Modeling and Choice of Appropriate Monitoring Parameters," AVT Symposium on Monitoring and Management of Gas Turbine Fleets for Extended Life and Reduced Costs, Manchester, UK, Oct. 8–11, pp. 9–1–9–13.
 [9] Provost, M. J., 2003, Observability Analysis for Successful Diagnosis of Gas Turbine Faults (VKI Lecture Series—Gas Turbine Condition Monitoring and Fault Diagnosis), von Karman Institute, Sint-Genesius-Rhode, Belgium.
 [10] Jasmani, M. S., Li, Y. G., and Ariffin, Z., 2010, "Measurement Selection for Multi-Component Gas Path Diagnostics Using Analytical Approach and Measurement Subset Concept," *ASME Paper No. GT2010-22402*.
 [11] Mushini, R., and Simon, D., 2005, "On Optimization of Sensor Selection for Aircraft Gas Turbine Engines," 18th International Conference on Systems Engineering (ICSEng 2005), Washington, DC, Aug. 16–18.
 [12] Borguet, S., and Leonard, O., 2008, "The Fisher Information Matrix as a Relevant Tool for Sensor Selection in Engine Health Monitoring," *Int. J. Rotating Mach.*, **2008**(1), p. 784749.
 [13] Santi, L., Sowers, T., and Aguilar, B., 2005, "Optimal Sensor Selection for Health Monitoring Systems," *AIAA Paper No. 2005-4485*.
 [14] Borguet, S., and Leonard, O., 2010, "A Sparse Estimation Approach to Fault Isolation," *ASME J. Gas Turbines Power*, **132**(2), p. 021601.
 [15] Litt, J., 2008, "An Optimal Orthogonal Decomposition Method for Kalman Filter-Based Turbofan Engine Thrust Estimation," *ASME J. Gas Turbines Power*, **130**(1), p. 011601.
 [16] Tang, H. L., and Zhang, J., 1999, "A Study of Object-Oriented Approach for Aero-Engine Performance Simulation," *J. Aerosp. Power*, **14**(4), pp. 421–424.
 [17] Chen, M., Tang, H. L., and Zhang, K., 2012, "Turbine Based Combined Cycle Propulsion System Integration Concept Design," *Proc. Inst. Mech. Eng., Part G*, **227**(7), pp. 1068–1089.
 [18] Pinelli, M., and Spina, P., 2002, "Gas Turbine Field Performance Determination: Sources of Uncertainties," *ASME J. Gas Turbines Power*, **124**(1), pp. 155–160.
 [19] Aretakis, N., Mathioudakis, K., and Stamatias, A., 2003, "Non-Linear Engine Component Fault Diagnosis From a Limited Number of Measurements Using a Combinatorial Approach," *ASME J. Gas Turbines Power*, **125**(4), p. 041701.
 [20] Golub, H. G., and Van, C. F., 1996, *Matrix Computations*, 3rd ed., John Hopkins University Press, Baltimore, MD.
 [21] Stamatias, A., Mathioudakis, K., Berios, G., and Papailiou, K. D., 1989, "Jet Engine Fault Detection With Discrete Operating Points Gas Path Analysis," 9th International Symposium on Air Breathing Engines, Athens, Sept. 3–8, ISABE Paper No. 89-7133.
 [22] Srinivas, M., and Patnaik, L. M., 1994, "Adaptive Probabilities of Crossover and Mutations in Gas," *IEEE Trans. SMC*, **24**(4), pp. 656–667.
 [23] Li, Y. G., 2008, "An Genetic Algorithm Approach to Estimate Performance Status of Gas Turbine," *ASME Paper No. ASME GT2008-50175*.
 [24] Gulati, A., Zedda, M., and Singh, R., 2000, "Gas Turbine Engine and Sensor Multiple Operating Point Analysis Using Optimization Techniques," *AIAA Paper No. 2000-3716*.
 [25] Li, Y. G., and Nilkitsaranont, P., 2009, "Gas Turbine Performance Prognostic for Condition-Based Maintenance," *Appl. Energy*, **86**(1), pp. 2152–2161.